Available online at www.sciencedirect.com

SCIENCE DIRECT®

Topology and its Applications 141 (2004) 59–85

Topology and its Applications

www.elsevier.com/locate/topol

Knot Floer homology, genus bounds, and mutation

Peter Ozsváth [a,*], Zoltán Szabó [b]

[a] *Department of Mathematics, Columbia University, New York 10027, USA*
[b] *Department of Mathematics, Princeton University, New Jersey 08540, USA*

Received 15 May 2003; received in revised form 1 September 2003

Abstract

In an earlier paper, we introduced a collection of graded Abelian groups $\widehat{HFK}(Y,K)$ associated to knots in a three-manifold. The aim of the present paper is to investigate these groups for several specific families of knots, including the Kinoshita–Terasaka knots and their "Conway mutants". These results show that $\widehat{HFK}$ contains more information than the Alexander polynomial and the signature of these knots; and they also illustrate the fact that $\widehat{HFK}$ detects mutation. We also calculate $\widehat{HFK}$ for certain pretzel knots, and knots with small crossing number ($n \leqslant 9$). Our calculations give obstructions to certain Seifert fibered surgeries on the knots considered here.

1. Introduction

In [18], we defined an invariant for knots $K \subset S^3$, which take the form of a graded Abelian group $\widehat{HFK}(K,i)$ for each integer i. The main results of [17] give explicit descriptions of some of the input required for determining $\widehat{HFK}$ in terms of the combinatorics of a generic planar projection of K. As an application, it is shown that $\widehat{HFK}$ for an alternating knot is explicitly determined by the Alexander polynomial and the signature of the knot (compare also [21]). The aim of the present article is to apply and extend techniques from [17] to determine certain knot homology groups of some more complicated types of knots. Indeed, to underscore the relative strength of $\widehat{HFK}$ over the Alexander polynomial, we focus mainly on certain knots with trivial Alexander polynomial (and hence vanishing signature).

* Corresponding author.
E-mail addresses: petero@math.columbia.edu (P. Ozsváth), szabo@math.princeton.edu (Z. Szabó).

0166-8641/$ – see front matter
doi:10.1016/j.topol.2003.09.009

These calculations have the following consequences. Of course, they show that $\widehat{HFK}$ is stronger than the Alexander polynomial; but more interestingly, they also show that, unlike many other knot invariants, $\widehat{HFK}$ is sensitive to Conway mutation. These computations further underline an interesting relationship between the knot Floer homology and the Seifert genus $g(K)$ of the knot K. Specifically, recall that in Theorem 5.1 of [18], we proved an adjunction inequality, stating that if $\deg \widehat{HFK}(K)$ denotes the largest integer d for which $\widehat{HFK}(K,d) \neq 0$, then

$$\deg \widehat{HFK}(K) \leqslant g(K). \tag{1}$$

Indeed, we also conjectured, based on the analogy with Seiberg–Witten theory and a theorem of Kronheimer and Mrowka [9], that

$$\deg \widehat{HFK}(K) = g(K)$$

for every knot in S^3. Calculations from this paper can be taken as further evidence supporting this conjecture.

Finally, the calculations provide obstructions to realizing Seifert fibered spaces as certain surgeries on S^3 along many of the knots studied here.

We emphasize that in general, calculating $\widehat{HFK}$ is not a purely combinatorial matter. The generators of this complex can be described combinatorially, and indeed in [17], we indentified them with Kauffman states (cf. [6]), but the differentials count pseudo-holomorphic disks in a symmetric product. However, there are some additional combinatorial aspects of this chain complex described below (see Section 2), including a multi-filtration on the chain complex, which facilitate our calculations. As a further illustration of these techniques, we also calculate the knot Floer homology groups for all knots with at most nine crossings.

We now give a description of the knots we study and state the results of our calculations.

1.1. Kinoshita–Terasaka and Conway knots

In [8], Kinoshita and Terasaka construct a family of knots $KT_{r,n}$, indexed by integers $|r| \neq 1$ and n, with trivial Alexander polynomial. These knots are obtained by modifying a picture of the $(r+1, -r, r, -r-1)$ (four-stranded) pretzel links, and introducing $2n$ twists. There are some redundancies in these knots. When $r \in \{0, 1, -1, -2\}$ or $n = 0$, this construction gives the unknot. Also, there is a symmetry identifying $KT_{r,n} = KT_{-r-1,n}$, which can be realized by turning the knot inside out. Finally, the reflection of $KT_{r,n}$ is the knot $KT_{r,-n}$. Now, recall that the knot Floer homology groups transform in a controlled manner under reflection: i.e., if $\overline{K}$ denotes the reflection of K, then for each $i, d \in \mathbb{Z}$,

$$\widehat{HFK}_d(K,i) \cong \widehat{HFK}^{-d}(\overline{K}, -i)$$

(where here the left-hand side denotes knot Floer homology in dimension d, while the right-hand side denotes knot Floer *co*-homology in dimension $-d$) and also

$$\widehat{HFK}_d(K,i) \cong \widehat{HFK}_{d-2i}(K,-i) \tag{2}$$

(cf. Eqs. (2) and (3), respectively, of [18]), so there is no loss of generality in assuming $r > 1$ and $n > 0$. We have illustrated the case where $r = 3$ and $n = 2$ in Fig. 1. It is possible

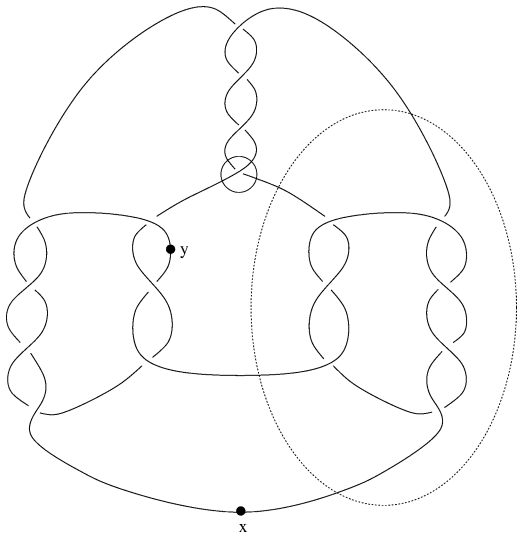

Fig. 1. *Kinoshita–Terasaka knot with* $r = 3$ *and* $n = 2$. When the circled crossing is changed, we obtain $KT_{3,1}$, while if it is resolved, we obtain a $(r+1, -r, r, -r-1)$-pretzel link. The Conway knot is obtained as a mutation around the sphere indicated here with a large, dotted ellipse (indeed, it is the mutation induced by 180° rotation about the axis perpendicular to the plane of the knot projection). The relevance of the indicated points x and y will become apparent in Sections 3 and 4, respectively.

to eliminate one crossing from the diagram for $KT_{r,n}$, but the new diagram is somewhat more cumbersome to draw.

We calculate the topmost non-trivial knot Floer homology group for $KT_{r,n}$ in Section 3, arriving at the following result:

Theorem 1.1. *Consider the Kinoshita–Terasaka knot* $KT_{r,n}$ *with* $n > 0$ *and* $r > 1$. *This knot has* $\widehat{HFK}(KT_{r,n}, s) = 0$ *for all* $s > r$, *and*

$$\widehat{HFK}(KT_{r,n}, r) \cong \mathbb{Z}^n_{(r)} \oplus \mathbb{Z}^n_{(r+1)},$$

where here (*and indeed throughout this paper*) *the subscript* (r) *indicates that the corresponding summand is supported in dimension* r.

Note that in [4], Gabai exhibits a Seifert surface for $KT_{r,n}$ with genus r, and proves that it is genus-minimizing, using the theory of foliations. It is interesting to note that Theorem 1.1, together with Inequality (1), gives an alternate proof that this Seifert surface is genus-minimizing. Some new applications will be described later (cf. Section 1.4).

Theorem 1.1 is based on the results of [17], where we give combinatorial descriptions of some of the data for calculating $\widehat{HFK}$. In fact, in Section 2 we explain how some of this data can be simplified, and amplify it with a multi-filtration on the chain complex of Kauffman states. Using these techniques, we obtain some additional calculations, as well.

Let $C_{r,n}$ denote the Conway knot, which is obtained from $K_{r,n}$ by mutation. This knot is obtained using the same construction as $K_{r,n}$, only using a four-stranded pretzel link of

type $(r+1,-r,-r-1,r)$ instead of $(r+1,-r,r,-r-1)$. Alternatively, it can be thought of as obtained from $K_{r,n}$ by a mutation using the sphere pictured in Fig. 1, cf. [10]. These knots also have trivial Alexander polynomial, and indeed, they satisfy the same symmetries as $K_{r,n}$. Note that these knots, too, admit a projection with one fewer crossing. In the case where $r=2$ and $n=1$, an eleven-crossing projection is pictured in Fig. 5. We prove the following in Section 4:

Theorem 1.2. *Let $C_{r,n}$ denote the Conway mutant of $KT_{r,n}$ with $n>0$ and $r>1$. This knot has $\widehat{HFK}(C_{r,n},s)=0$ if $s>2r-1$, and*

$$\widehat{HFK}(C_{r,n},2r-1)\cong\mathbb{Z}^n_{(2r-1)}\oplus\mathbb{Z}^n_{(2r)}.$$

It is easy to construct Seifert surfaces F for $C_{r,n}$ with genus $g(F)=2r-1$, compare [3], see also Section 4.

Since $KT_{r,n}$ and $C_{r,n}$ differ by a Conway mutation, and their groups $\widehat{HFK}$ are manifestly different, we see that, unlike the Alexander, Jones, HOMFLY, and Kauffman polynomials, the invariant $\widehat{HFK}$ is sensitive to mutation. It is interesting to compare this with Khovanov's invariants, cf. [23,7].

1.2. Pretzel knots

The techniques described here also lend themselves quickly to a calculation for pretzel knots $P(p,q,r)$, where p, q, and r are odd integers. When p, q, and r all have the same sign, these knots are alternating, and hence their Floer homology has been determined in [17]. Thus, by reflecting the knot if necessary and relabeling, we are left with the case where $q<0$ and $p,r>0$.

Theorem 1.3. *Consider the knot $K=P(p,q,r)$ where $p=2a+1$, $q=-(2b+1)$, $r=2c+1$, with $a,b,c\geqslant 0$. Then, if $b\geqslant\min(a,c)$, we have that*

$$\widehat{HFK}(K,1)=\mathbb{Z}^{ab+bc+b-ac}_{(1)}.$$

If $b<\min(a,c)$, we have that

$$\widehat{HFK}(K,1)=\mathbb{Z}^{b(b+1)}_{(1)}\oplus\mathbb{Z}^{(b-a)(b-c)}_{(2)}.$$

This family contains infinitely many knots with trivial Alexander polynomial: the Alexander polynomial is trivial precisely when $pq+qr+pr+1=0$ (e.g., let $(p,q,r)=(-3,5,7)$). It follows at once from the above theorem that for all non-trivial pretzel knots in the above family, $\widehat{HFK}$ is also non-trivial.

1.3. Knots with few crossings

Although the techniques from Section 2 are not sufficient to calculate $\widehat{HFK}$ in general, they can be employed successfully in the study of relatively small knots, as measured by the number of double-points. In fact, in Section 6 we calculate $\widehat{HFK}$ for all knots with

nine or fewer crossings, except for two particular knots whose $\widehat{HFK}$ has been calculated in [18] and [16] (the knot 9_{42} and 8_{19}—the $(3,4)$ torus knot). The Floer homology of the remaining non-alternating knots (with less than ten crossings) behaves like the Floer homology of alternating knots, cf. Theorem 6.1 below.

1.4. Surgeries on knots

In another direction, the calculations of this paper can be used to give information on three-manifolds obtained as integral surgeries on knots, following results of [19] (see also [20]). To explain, recall that the formal sum of Euler characteristics of $\widehat{HFK}$ gives the symmetrized Alexander polynomial $\Delta_K(T)$:

$$\sum_i \chi\big(\widehat{HFK}(K,i)\big)\cdot T^i = \Delta_K(T) \tag{3}$$

(cf. Section 10 of [18]). It is an immediate corollary of this that

$$\deg \Delta_K \leqslant \deg \widehat{HFK}(K). \tag{4}$$

It is a result of [19] (see especially Corollary 1.5 of [19]) that if K is a knot for which $\deg \widehat{HFK}(K) > 1$ and Inequality (4) is strict, then K does not admit certain Seifert fibered surgeries. Specifically, we have the following:

Corollary 1.4. *For any integer $q \neq 0, 1/q$ surgery on S^3 along $KT_{n,r}$ or $C_{n,r}$ (with $n > 0$ and $r > 1$) is never Seifert fibered space.*

For the case of pretzel knots $P(p,q,r)$ with p, q, and r all odd, Corollary 1.5 of [19] no longer applies, since $\deg \widehat{HFK}(K) = 1$. And indeed, there are cases of such pretzel knots with Seifert fibered surgeries. However, a careful look at the proof of that corollary, and a closer look at $\widehat{HFK}$ gives the following corollary (cf. Proposition 5.6). Note that this corollary covers all non-trivial three-stranded pretzel knots with trivial Alexander polynomial (compare with [5,11]):

Corollary 1.5. *Let $P(p,q,r)$ be a non-trivial pretzel knot with p, q, and r odd. When $p \geqslant r > 0$ and $q < -1$ with $|q| < \min(p-2, r)$, no integral surgery along $P(p,q,r)$ is a Seifert fibered space.*

Further remarks. Additional calculations of knot Floer homology groups can be found in [22] and [2]. The authors wish to thank Eaman Eftekhary, Cameron Gordon, Mikhail Khovanov, Rob Kirby, Paul Melvin, and Jacob Rasmussen for interesting conversations.

2. Calculational tools

Let $K \subset S^3$ be a knot. In [18], we introduced the knot Floer complex $\widehat{CFK}(K) = \bigoplus_{s\in\mathbb{Z}} \widehat{CFK}(K,s)$ which is associated to a Heegaard diagram for a knot, and whose

homology groups are knot invariants, see also [22]. In [17], we gave a description of the generators of the chain complex $\widehat{CFK}$ in terms of combinatorics of a generic projection for a knot (together with some extra data). We recall the constructions in Section 2.1, and show that in some cases, the number of generators can be cut down, to make the calculations simpler. In Section 2.2, we give a combinatorial description of the domain of a homotopy class $\phi \in \pi_2(\mathbf{x}, \mathbf{y})$ connecting a pair of states. Here, the condition that $\mathcal{D}(\phi) \geqslant 0$ from [14] (a necessary condition for $\mathbf{y}$ to appear with non-zero multiplicity in the expression for $\partial\mathbf{x}$) is formulated in terms of a multi-filtration on the set of states.

In Section 2.3, we recall the correspondence between states and maximal subtrees (see also [6]), which removes much of the redundancy which is inherent in the description of a state.

In Section 2.4, we turn to certain properties of the "skein exact sequence" from [18].

2.1. Simplifying Heegaard diagrams

Choose an orientation for K and a generic projection of K to the plane. The projection gives a planar graph G where the vertices of G correspond to the double-points of the projection of K, and the edges inherit an orientation from K. Choose a distinguished edge ε_0 for this planar graph. We call a projection with this additional data a *decorated knot projection*.

There are four distinct quadrants (bounded by edges) emanating from each vertex, each of which is a corner of the closure of some region of $S^2 - G$. We distinguish the two of these regions which contain the distinguished edge on their boundary, denoting them **A** and **B**.

Definition 2.1. A *state* (cf. [6]) is an assignment which associates to each vertex of G one of the four in-coming quadrants, so that:

- the quadrants associated to distinct vertices are subsets of distinct regions in $S^2 - G$,
- none of the quadrants associated to vertices is a corner of the distinguished regions **A** or **B**.

It is easy to see that a state sets up a one-to-one correspondence between vertices of G and the regions of $S^2 - G - \mathbf{A} - \mathbf{B}$.

Definition 2.2. The *filtration level* of a state is the integer obtained by adding up the local contributions at each quadrant, which are determined by the crossing types of the knots, as indicated in Fig. 2. The *absolute grading* of a state is determined by adding up another local contribution, pictured in Fig. 3.

We have the following result from [17]:

Theorem 2.3. *Fix a generic knot projection for a knot $K \subset S^3$. There is a one-to-one correspondence with generators of $\widehat{CFK}(K, i)$ and states x whose associated filtration*

Fig. 2. *Local filtration level contributions*. We have illustrated the local contributions for the filtration level of a state for both kinds of crossings.

Fig. 3. *Local grading contributions*. We have illustrated the local contribution for the absolute grading associated for a state.

level is i. Under this correspondence, the absolute grading of a state in the above sense coincides with the absolute degree of the corresponding generator of $\widehat{CFK}(K,i)$.

Definition 2.4. Fix a decorated knot projection. An *essential interval* is a sequence of consecutive edges with the following properties:

- the distinguished edge ε_0 appears in the sequence, so we can write
$$E = \bigcup_{i=-\ell}^{m} \varepsilon_i,$$
where here $\ell, m \geqslant 0$, and ε_{i+1} is the successor of ε_i for all $i = -\ell, \ldots, m-1$,
- the immersed arcs
$$E_+ = \bigcup_{i=1}^{m} \varepsilon_i \quad \text{and} \quad E_- = \bigcup_{i=-\ell}^{-1} \varepsilon_i$$
are pairwise disjoint,
- as we traverse the arc E_+ according to the orientation of K, i.e., starting at the vertex $\varepsilon_0 \cap \varepsilon_1$, and then passing through $\varepsilon_1, \ldots, \varepsilon_m$ in order, all of the crossings we encounter for the first time have the same type (i.e., they are all either over- or under-crossings); similarly, as we traverse the arc E_- backwards, i.e., starting at $\varepsilon_0 \cap \varepsilon_{-1}$, and proceeding through till $\varepsilon_{-\ell}$, all the crossings we encounter the first time have the same type (which might be different from the crossing type encountered along E_+).

Definition 2.5. Fix a decorated knot projection, and also an essential interval $E = \bigcup_{i=-\ell}^{m} \varepsilon_i$. Each edge ε_i inherits an orientation from K, and we write its endpoints as

$\partial\varepsilon_i = v_{i+1} - v_i$, so that $\{v_{-\ell}, \dots, v_{m+1}\}$ are the vertices in the order they appear along E. An E-essential state is a state x with the following properties:

- for $i = 1, \dots, m$, if $v_i \notin \{v_1, v_2, \dots, v_{i-1}\}$, then the corner containing $x(v_i)$ contains the edge ε_i on its boundary;
- for $i = -\ell + 1, \dots, 0$, if $v_i \notin \{v_0, v_{-1}, \dots, v_{i+1}\}$, then the corner containing $x(v_i)$ contains the edge ε_{i-1} on its boundary.

Proposition 2.6. *Fix a knot projection G for a knot $K \subset S^3$, and let E be an essential arc. Then, there is a system of generators for $\widehat{CFK}$ consisting of only E-essential states* (*in the sense of Definition* 2.5)*, with gradings and filtration levels as given in Theorem* 2.3.

Proof. Recall that the Heegaard surface constructed in [17] is obtained as a boundary regular neighborhood of the knot projection. For each vertex v, we have a β-curve denoted β_v, and at the distinguished ε_0, we choose a meridian μ for the knot which is supported near ε_0. Then, on either side of that meridian in the Heegaard surface, we choose a pair of basepoints w and z for the definition of $\widehat{CFK}(K)$.

Suppose for simplicity that all the v_i are distinct (i.e., that $E_- \cup E_+$ is an embedded arc in G). To simplify the Heegaard diagram as above, we move the two basepoints further away from the meridian, so that we can handleslide the β-curves belonging to v_1 and v_0 across μ, to get new curves β_1' and β_0'. We continue handlesliding in this manner—$\beta_{v_{k+1}}$ across β'_{v_k} and $\beta_{v_{-k}}$ across $\beta'_{v_{-k+1}}$—until we have a new sequence of β-curves $\beta'_{v_0}, \dots, \beta'_{v_k}$ which now meet always at most two α-curves (rather than four). The hypothesis on the crossing types was used to ensure that the reference points could always be moved out of the handlesliding region (without crossing any of the attaching circles). This procedure is illustrated in Fig. 4. It is not difficult to modify the above procedure when E_- and E_+ have self-intersections. □

Of course, the notion of essential arc, and the above proposition depends on the choice of essential interval. However, for some decorated knot projections, there is always a unique maximal essential interval. Indeed, this is the case for all the projections we consider in this paper, and hence, with this understood, we call a state an essential state if it is E-essential for this maximal essential interval E.

2.2. The combinatorics of domains, and the multi-filtration

Of course, the calculation of $\widehat{HFK}(K)$ requires an explicit understanding of the differential in the complex $\widehat{CFK}(K)$, which in turn involves a pseudo-holomorphic curve count. More precisely, given a pair of states x and y (whose filtration level coincides, and whose absolute gradings differ by one), letting $\mathbf{x}$ and $\mathbf{y}$ denote the corresponding generators of $\widehat{CFK}(K)$, there is a unique homotopy class of Whitney disk $\phi \in \pi_2(\mathbf{x}, \mathbf{y})$ with $n_z(\phi) = n_w(\phi) = 0$. The $\mathbf{y}$ component of $\partial\mathbf{x}$ is the signed count of points $\#\mathcal{M}(\phi)/\mathbb{R}$ in the moduli space of pseudo-holomorphic representatives of ϕ (modulo translation). At present, this count does not have a direct combinatorial description. However, there are combinatorial conditions on x and y which ensure that it vanishes.

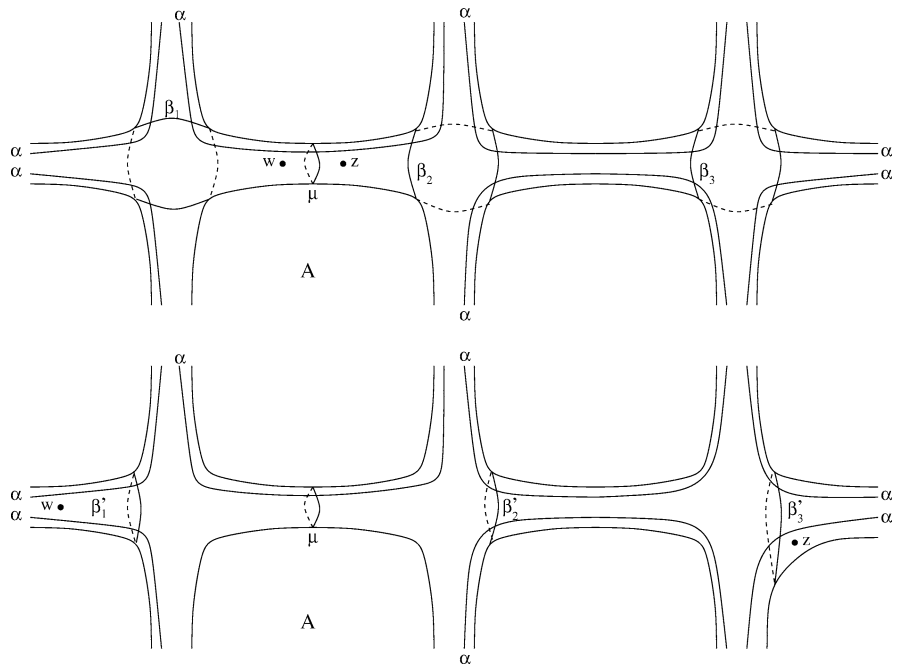

Fig. 4. *Diagram simplification*. We have illustrated the proof of Proposition 2.6. At the top, we have illustrated the part of the Heegaard diagram coming from [17] (near where we have two under-crossings followed by one over-crossing), choosing our reference point between the under- and the over-crossing. We have dropped all the subscripts to the α-curve, but we remind the reader that there is one region in each of the compact components of $\mathbb{R}^2 - G$ (the non-compact region here is denoted by **A**). At the bottom, we have illustrated the corresponding "simplification".

Let G be a graph for the knot projection of K with N edges. We order the edges $\{\varepsilon_i\}_{i=0}^{N-1}$ of G, so that ε_0 is the marked edge, and the others appear in the order in which they are encountered by moving along K (with its specified orientation). Let v_i denote the vertex at the intersection of ε_i with ε_{i+1} (note that each vertex in G appears as v_i for two different values of i, once as an overcrossing, and once as an undercrossing). We can associate to each state x a multi-filtration-level

$$M_x \in \mathrm{Hom}\big(\{\varepsilon_i\}_{i=0}^{N-1}, \mathbb{Z} \oplus \mathbb{Z}\big),$$

as follows:

$$M_x(\varepsilon_i) = \begin{cases} (0,0) & \text{if } i = 0, \\ M_x(\varepsilon_{i-1}) + (0,1) & \text{if } v_i \text{ is an overcrossing and } x(v_i) \text{ is to the right of } \varepsilon_i \cup \varepsilon_{i-1}, \\ M_x(\varepsilon_{i-1}) - (0,1) & \text{if } v_i \text{ is an overcrossing and } x(v_i) \text{ is to the left of } \varepsilon_i \cup \varepsilon_{i-1}, \\ M_x(\varepsilon_{i-1}) + (1,0) & \text{if } v_i \text{ is an undercrossing and } x(v_i) \text{ is to the left of } \varepsilon_i \cup \varepsilon_{i-1}, \\ M_x(\varepsilon_{i-1}) - (1,0) & \text{if } v_i \text{ is an undercrossing and } x(v_i) \text{ is to the right of } \varepsilon_i \cup \varepsilon_{i-1}. \end{cases}$$

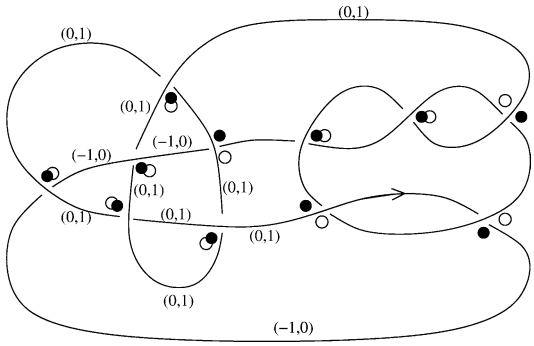

Fig. 5. *A domain*. Let x denote the state indicated by the dark circles and y denote the state indicated by the hollow ones, in the Conway knot as pictured above. Then, $\frac{1}{2}(M_x - M_y)$ is represented as above: specifically, near each edge ε, we have written $\frac{1}{2}(M_x - M_y)(\varepsilon)$, unless the latter quantity vanishes. Since sometimes this is negative, it follows that $x \not> y$, and hence, although it is easy to see that $\deg(x) = \deg(y) + 1$, y does not appear in the expansion for ∂x.

Definition 2.7. Fix a decorated knot projection. We define a partial ordering on the set of states, as follows: if x and y are two different states, then $x > y$ if for all edges ε, $M_x(\varepsilon) - M_y(\varepsilon)$ is a pair of non-negative integers.

An example of two states x and y for which $x \not> y$ and $y \not> x$ is illustrated in Fig. 5.

Proposition 2.8. *Suppose that x and y represent the same filtration level, and indeed suppose that y appears in ∂x with non-zero multiplicity, then $x > y$.*

Proof. Let $(\Sigma, \boldsymbol{\alpha}, \boldsymbol{\beta})$ denote the Heegaard diagram for S^3 used for Theorem 2.3. Consider an edge ε_i in the knot projection which does not meet the one of the two distinguished regions in the knot diagram. This edge, then, gives rise to a cylinder in the Heegaard diagram, which is divided into two squares by the α-arcs. We place one reference point t_i in the "top" part of the diagram, and another one b_i in the "bottom" part. It is easy to see (after a straightforward case-by-case analysis of $x(v_i)$ and $y(v_i)$) that if $\phi \in \pi_2(\mathbf{x}, \mathbf{y})$ is the homotopy class with $n_z(\phi) = n_w(\phi) = 0$, then

$$\frac{1}{2}\big(M_x(\varepsilon_i) - M_y(\varepsilon_i)\big) = \big(n_{t_i}(\phi), n_{b_i}(\phi)\big).$$

The result now follows from the basic fact that if ϕ has a pseudo-holomorphic representative (for suitably small perturbations of the holomorphic condition), then all these multiplicities must be non-negative (cf. Lemma 3.2 of [14]).

Note that this argument also applies when the Heegaard diagram is "simplified" as in Proposition 2.6, only in that case, one uses the multi-filtration only over those edges which are not in the essential interval.

2.3. Trees

States admit a rather economical description in graph-theoretic terms (see also [6]). The regions in the complement of the planar projection can be colored black and white in a

chessboard pattern, by the rule that any two regions which share an edge have opposite color. There is then an associated "black graph", whose vertices correspond to the regions colored black, and whose edges correspond to vertices in G, which connect the opposite black regions. We let **A** (respectively **B**) denote the black (respectively white) region whose boundary contains the distinguished edge ε_0.

In these terms, states are in one-to-one correspondence with the maximal subtrees of the black graph. Given a state x, we associate to it the union of vertices of G, thought of now as edges in the black graph, to which x associates a black quadrant. This gives the maximal black subtree associated to the state x.

Conversely, given a black subtree T, we can orient the edges so that the "root" is the distinguished black region **A**, and all edges point away from this root. We construct the black part of the corresponding vertex assignment, as follows. Let v be a vertex of G which corresponds to some edge of T. With respect to the induced orientation on T, this oriented edge of T points to a uniquely determined endpoint $r \in T$, which in turn corresponds to one of the two black quadrants (in $S^2 - G$) which meet at v. We let $x(v)$, then, be the quadrant corresponding to r. To determine the rest of the vertex assignment, we first consider the dual white graph T^*, obtained from the white graph by deleting all the edges corresponding to the vertices appearing in the black subtree T. Note that T^* is actually a tree, and repeat the above procedure, now for the white quadrants.

Clearly, one can reformulate the results of Theorem 2.3 in terms of these graphs. Each edge of both the black and white graphs inherits a label among the numbers $\{-1, 0, +1\}$: an edge in the white (respectively black) graph is labelled with 0 if the two white (respectively black) quadrants meeting at the corresponding vertex both are have grading contribution 0 (cf. Fig. 3), and it is labelled with ± 1 if one of the two white (respectively black) graph is labelled with ± 1. We call edges labelled with 0 *neutral* edges, and view them as unoriented, while the non-neutral ones are oriented (so as to point away from the vertex corresponding to the quadrant labelled with 0 in Fig. 3).

Given a black tree T, let T^* be its dual white tree, and orient both as before (so that the edges of T and T^* point away from **A** and **B**, respectively). Then, twice the filtration level corresponding to T is obtained as follows. We sum over all edges e in T the label of the edge e in G times $+1$ if its orientation as an edge of the black graph agrees with the induced orientation coming from T, and -1 if the orientations disagree (note here that this last sign is irrelevant for neutral edges); and then add to that the corresponding sum for all edges of the dual white graph T^*.

Similarly, the grading level corresponding to T is obtained by summing over all edges e in T the label of the edge e in G, provided that its orientation agrees with the induced orientation coming from T (and zero otherwise), and once again adding the corresponding sum for T^*.

2.4. Exact sequences

In a different direction, we derived in [18] a "skein exact sequence", which we recall here.

Suppose that K is an oriented knot in Y, and we have a disk D which meets K in two algebraically cancelling points. If we perform -1 surgery on $\gamma = \partial D$, we obtain a new knot

K_- in S^3, which is obtained from K by introducing a full twist in a tubular neighborhood along γ. Performing $+1$ surgery on γ gives us another knot K_+ with a full twist introduced in the other direction. There is a third link K_0 which is obtained by resolving the knot (so as to miss D entirely). Recall [18] that the link invariant in this case is, by definition, the knot invariant for the knot in $S^1 \times S^2$ obtained by performing a zero-surgery along γ.

In [18], we established skein exact sequences for each integer i

$$\cdots \to \widehat{HFK}(K,i) \xrightarrow{f_1} \widehat{HFK}(K_0,i) \xrightarrow{f_2} \widehat{HFK}(K_+,i) \xrightarrow{f_3} \cdots$$

and

$$\cdots \to \widehat{HFK}(K_-,i) \xrightarrow{g_1} \widehat{HFK}(K_0,i) \xrightarrow{g_2} \widehat{HFK}(K,i) \xrightarrow{g_3} \cdots,$$

where the maps f_i and g_i are induced by two-handle additions.

It will be useful to us to have the following compatibility result about g_2 and f_1:

Lemma 2.9. *For the above two exact sequences, the composite*

$$g_2 \circ f_1 : \widehat{HFK}(K,i) \to \widehat{HFK}(K,i)$$

is trivial.

Proof. The map f_1 is induced by cobordism formed by zero-surgery on γ, while g_2 is induced by the cobordism formed by zero-surgery on another unknot δ which links γ once (and does not link the knot K). As in [15], we obtain the same map if we switch the order in which we perform the two two-handle additions: first we perform zero-surgery on δ, and then zero-surgery on γ (see Fig. 6). However, in this latter ordering, we factor through the three-manifold $Y \# (S^2 \times S^1)$ (and the knot is contained entirely in the Y summand. It is easy to adapt the Künneth principle for connected sums in this context (see especially Proposition 6.1 of [13]) to see that

$$\widehat{HFK}\big(Y \# \big(S^2 \times S^1\big), K, i\big) \cong \widehat{HFK}(Y,K,i) \otimes H^1\big(S^2 \times S^1\big). \tag{5}$$

Of course, $H^1(S^2 \times S^1) \cong \mathbb{Z} \oplus \mathbb{Z}$, but our reason for writing the answer in this form is that we have now an action of $[\delta] \in H_1(S^2 \times S^1)$ on $\widehat{HFK}(Y \# (S^2 \times S^1), i)$ (induced from the corresponding action on $\widehat{HF}(Y \# (S^2 \times S^1))$). The above isomorphism is compatible with this action of $[\delta]$ (where $[\delta] \in H_1(S^2 \times S^1)$ acts on the right-hand side through its natural action on $H^1(S^2 \times S^1)$, cf. Section 4.2.5 of [14]). Now, f_1 maps to the kernel

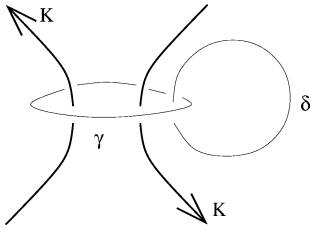

Fig. 6. *Composite map*. We have pictured here two strands of K. Performing zero-surgery on γ realizes the map f_1, while zero-surgery on δ realizes g_2.

of the $[\delta]$-action, since the curve representing δ is null-homologous in the four-manifold obtained by attaching a two-handle along δ to $Y - K$; while g_2 is trivial on the image of the $[\delta]$-action because, once again, δ is null-homologous in the corresponding four-manifold (compare [15]). But in the description of the $[\delta]$-action from Eq. (5), it is clear that the image of $[\delta]$ coincides with the kernel of $[\delta]$, completing the proof. □

3. Calculations for the Kinoshita–Terasaka knots

Consider the Kinoshita–Terasaka knots $KT_{r,n}$ with $n \neq 0$. All the knots $KT_{r,n}$ have trivial Alexander polynomial, but the knots themselves are non-trivial when $r > 1$ and $n \neq 0$. Indeed, Gabai exhibits a Seifert surface for $KT_{r,n}$ of genus r and proves (cf. [4]) that this Seifert surface has minimal genus.

We shall focus first on the case where $n = 1$. We distinguish the edge connecting the base of the $-r - 1$ and $r + 1$ strands opposite to where the $(n = 1)$ twisting takes place—this is indicated by the point x pictured in Fig. 1. We have illustrated the "black graph" of $KT_{r,1}$, in Fig. 7. For the black graph, there are two edges, labeled e and f, and four chains $\{a_i\}_{i=1}^{r+1}$, $\{b_i\}_{i=1}^{r}$, $\{c_i\}_{i=1}^{r}$ and $\{d_i\}_{i=1}^{r+1}$. The edges e, f, b_i, and d_i are labeled with $+1$, while

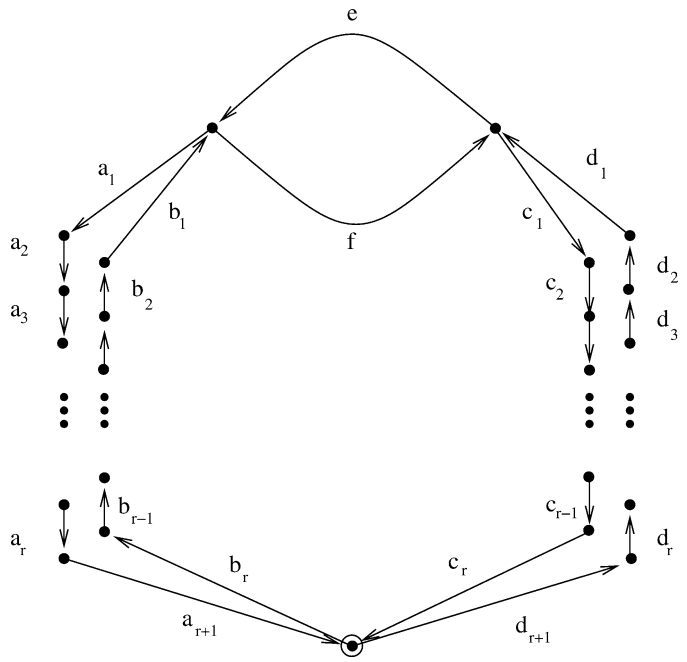

Fig. 7. *Black graph for the Kinoshita–Terasaka knot.* The following edges are labeled with $+1$: e, f $\{b_i\}_{i=1}^{r}$, $\{d_i\}_{i=1}^{r+1}$; the following are labeled with -1: $\{a_i\}_{i=1}^{r+1}$, $\{c_i\}_{i=1}^{r}$. The distinguished black vertex is circled. The white regions correspond to the complement of this graph in S^2, and the distinguished white region is the non-compact one (i.e., the one bounded by the chain of $\{a_i\}$, $\{d_i\}$, and e). Note that all the edges in the dual white graph are neutral (since none of the edges in the black graph are).

Fig. 8. *Generators for $K_{n,r}$ with $n = 1$, $r = 2$.*

those of type a_i and c_i are labeled with -1. The distinguished black region corresponds to the vertex where a_{r+1}, b_r, c_r, and d_{r+1} meet. The vertices of the white graph are, of course, the regions in the complement of this planar graph. The region bounded by the chain of b_i and c_i and the edge f corresponds to the distinguished white region. In fact, since none of the black edges is neutral, all of the white ones are.

We calculate $\widehat{HFK}(KT_{r,n}, r)$ in the case where $n = 1$ using Theorem 2.3, together with the multi-filtration (Proposition 2.8). The case where n is arbitrary will follow from properties of the skein exact sequence cf. Lemma 2.9 (though one could alternately give a more direct argument using the multi-filtrations).

Proof of Theorem 1.1 when $n = 1$. It is easy to see that there are two trees B and C which represent filtration level $-r$: the tree B does not contain a_{r+1}, f, c_r, or d_{r+1}, while the tree C does not contain a_{r+1}, e, b_r, or d_{r+1}. These trees are illustrated in Fig. 8.

Moreover, the grading of B is given by $1 - r$, while the grading of C is given by $-r$. It is straightforward to verify that $B \not\sim C$ for the multifiltration (see Fig. 9 for an illustration) and hence, according to Proposition 2.8, $\partial \equiv 0$. These calculations show that

$$\widehat{HFK}(KT_{r,1}, s) \cong \begin{cases} 0 & \text{if } s < -r, \\ \mathbb{Z}_{(-r)} \oplus \mathbb{Z}_{(1-r)} & \text{if } s = -r. \end{cases}$$

Note that this is equivalent to the statement of the theorem (with $n = 1$), in view of the symmetry of the knot Floer homology groups (cf. Eq. (2)).

Calculation for an $(r + 1, -r, r, -r - 1)$ pretzel link. Note that there is a skein exact sequences of the form

$$\cdots \to \widehat{HFK}(KT_{r,n-1}, i) \xrightarrow{f_1^n} \widehat{HFK}(X(r), i) \xrightarrow{f_2^n} \widehat{HFK}(KT_{r,n}, i) \to \cdots, \tag{6}$$

where $X(r)$ is an oriented $(r + 1, -r, r, -r - 1)$ pretzel link which is independent of n. (Strictly speaking, the notation for f_1^n and f_2^n ought to include the level i, but we suppress this for readibility.) The maps f_1^n and f_2^n both decrease absolute grading by $\frac{1}{2}$. In fact, according to Lemma 2.9,

$$f_2^n \circ f_1^{n+1} \equiv 0. \tag{7}$$

Moreover, $KT_{r,0}$ is the unknot. Specializing to the case where $i = r$, and $n = 1$ it follows at once that

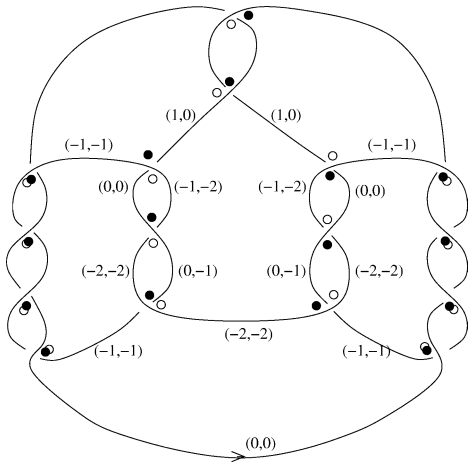

Fig. 9. *Comparison of generators B and C*. We have labeled some of the multiplicities for the multi-filtration comparing these two generators of $\widehat{HFK}(KT_{n,r}, -r)$, when $n = 1$ and $r = 2$. Here, B is denoted by the black dot, and C by the hollow one. The arrow appears on the distinguished edge of the knot projection (at the vertex denoted by x in Fig. 1).

$$\widehat{HFK}\big(X(r), r\big) \cong \mathbb{Z}_{(r-\frac{1}{2})} \oplus \mathbb{Z}_{(r+\frac{1}{2})}, \tag{8}$$

and the map f_2^1 is an isomorphism.

Proof of Theorem 1.1 for arbitrary *n*. To establish the theorem for all $n \geqslant 1$ we prove inductively both the theorem, and also the statement that the map f_2^n is injective. The basic case was established above. For the inductive step, if f_2^{n+1} is not injective, then f_1^{n+1} would have to be non-trivial, but this contradicts the injectivity of f_2^n (which holds by the inductive hypothesis), together with Lemma 2.9, in the form of Eq. (7).

3.1. Additional remarks

Consider the case of $K_{r,n}$ with $n = 1$. By moving the marked edge, we obtain various chain complexes representing $\widehat{HFK}(K_{r,1})$. Typically, subtrees which represent filtration level r vary as we move the marked edge. However, since the white graph consists of neutral edges only, if we choose our marked edge so that the distinguished black region X remains unchanged—there are four possible choices—then the maps from maximal subtrees to filtration levels and degrees are unchanged. However, the map from maximal subtrees to states, of course, varies, and more interestingly, the induced partial ordering on subtrees can change, too. For example, if we mark the edge of B opposite to the edge containing x (cf. Fig. 1), then it is easy to see that the two generators B and C described in the proof of Theorem 1.1 are still the two representatives for filtration level r, and their dimensions are $r + 1$ and r. However, with this choice of marked edge, it is now the case that $B > C$.

4. Calculations for the Conway knots

We consider the Conway mutants $C_{r,n}$ of the Kinoshita–Terasaka knots. The calculation of $\widehat{HFK}(C_{r,n}, 2r-1)$ proceeds similarly to the calculations from Section 3. Note that the knot $C_{2,1}$ can be given the eleven-crossing presentation pictured in Fig. 5. In this case, if we place the reference point where the arrow is indicated, and use the simplification of the Heegaard diagram described in Section 2, then it is straightforward to see that in filtration level 3 there are only two inessential states, the two states x and y pictured in the figure, and they have absolute grading 4 and 3, respectively. However, $\partial x = 0$, since $x \neq y$, as illustrated in the figure, verifying Theorem 1.2 for $r = 2$, $n = 1$.

As before, we begin by restricting to the case where $n = 1$. Rather than drawing the black graph in this case, we indicate the necessary modifications to Fig. 7. (Note that it is not hard to find projections with fewer essential states than the ones we describe—indeed, in the desired filtration level, we can arrange for there to be only two essential states, as in the case with $r = 2$ considered above. However the diagrams we describe presently have the advantage that they are easier to describe in words.) The black graph of $C_{r,n}$ looks just like that for $KT_{r,n}$, except that now there are $r+1$ edges of type c_i, and only r edges of type d_i. Moreover, the edges labeled with $+1$ are e, f, $\{b_i\}_{i=1}^{r}$ and $\{c_i\}_{i=1}^{r+1}$, and the edges labeled with -1 are $\{a_i\}_{i=1}^{r+1}$ and $\{d_i\}_{i=1}^{r+1}$. In particular all edges in the dual white graph remain neutral. We choose our marked edge to contain the point y in Fig. 1 (after mutating). Correspondingly, now, the distinguished black edge at the vertex between b_1 and b_2, and the distinguished white region is bounded by the chains $\{b_i\}_{i=1}^{r}$, $\{c_i\}_{i=1}^{r+1}$ and the edge f.

Lemma 4.1. *For the diagram of $C_{r,1}$ described here with $r > 2$, there are* 8 *Kauffman states representing filtration level* $2r-1$. *Of these,* 3 *are in dimension $r+2$, which we denote CE, CF_1, CF_2, and CF_3, and* 3 *are in dimension $r+1$, which we denote DE, DF_1 DF_2, and DF_3.* (*Note that these states are explicitly identified in the proof below, which also explains their notation. See also Fig.* 10.) *In the case where $r = 2$, we have only* 6 *essential states*: *the two states CF_1 and DF_1 are missing from this diagram.*

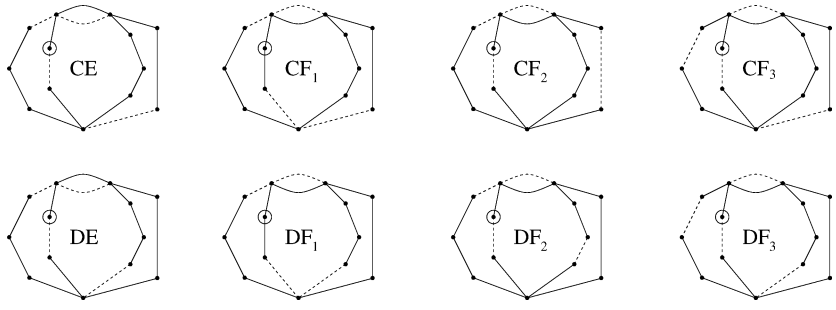

Fig. 10. *Generators for $C_{n,r}$ with $n = 1$, $r = 3$.*

Proof. Notice that there are a total of $4r+4$ edges in the black graph, and in fact a maximal spanning tree must contain exactly $4r$ edges. It is clear that a maximal tree which contains neither e nor f has filtration level at most r.

Thus, all maximal subtrees with filtration level $2r-1$ contain either e or f. Now, if T is a maximal subtree which contains one of E or F, then clearly, it must contain at least one of the chains $A=\{a_i\}$, $B=\{b_i\}$, $C=\{c_i\}$ or $D=\{d_i\}$. Indeed, it cannot contain more than one. Accordingly, we say that a tree is of type AE if it contains the chain A and the vertex e. We analyze the eight cases separately.

Trees of type AE which represent filtration level $2r-1$, we claim, cannot contain the edge b_1. But a tree which contains A, and does not contain b_1 corresponds to an inessential vertex assignment—and indeed, in the case where $r>2$, such trees never represent filtration level $2r-1$. The same remarks rule out trees of type AF, and similar remarks rule out trees of type BE, and BF.

It is easy to see that there is only one tree of type CE which represents filtration level $2r-1$, and it is the one which does not contain a_1, f, b_2, and d_r. Similarly, there is only one tree of type DE, and it does not contain a_1, f, b_2, and c_{r+1}.

Assume for the moment that $r>2$. There are three trees of type CF representing filtration level $2r-1$: one which does not contain e, a_1, b_3, and d_r, which we denote CF_1, one which does not contain e, a_1, b_2, and d_2, which we denote CF_2, and one which does not contain e, a_2, b_2, and d_r. Similarly, there are three trees of type DF representing filtration level $2r-1$, which we denote $\{DF_i\}_{i=1}^{3}$, where DF_i is gotten from CF_i by deleting e and c_{r+1} and adding f and d_r. The case where $r=2$ works similarly, except that the states CF_1 and DF_1 do not exist. □

Lemma 4.2. *Consider the essential generators listed in Lemma* 4.1 *for* $C_{r,1}$ *with* $r>2$. *These have the following ordering properties for the multi-filtration*:

$$\begin{aligned} &CF_1 > CF_2 > CE > CF_3, \\ &DF_1 > DF_2 > DE > DF_3, \end{aligned} \tag{9}$$

and

$$CF_3 \not> DE, \qquad CE \not> DF_2, \qquad CF_2 \not> DF_2. \tag{10}$$

Moreover, fixing fix $i \neq 2$, *and letting* $\phi \in \pi_2(CF_i, DF_i)$ *be the homotopy class with* $n_w(\phi)=0$, *we have that*

$$\#\left(\frac{\mathcal{M}(\phi)}{\mathbb{R}}\right)=1. \tag{11}$$

The same holds for the corresponding homotopy class in $\pi_2(CE, DE)$. *When* $r=2$, *the same remarks hold, excluding states* CF_1 *and* DF_1.

Proof. Verifying the order properties is straightforward. Some of the work in verifying relation (10) is shortened, given relation (9), and the observation that the difference in the multi-filtering between CF_i and DF_i for $i\neq 2$ is supported in a single edge; a similar remark holds for CE and DE. For the statement about homotopy classes, observe that all of these homotopy classes are represented by quadrilaterals, and hence $\#\mathcal{M}(\phi)/\mathbb{R}$ can be calculated by one-variable complex analysis (compare Section 3 of [13]). □

Proof of Theorem 1.2. Again, we start with the case where $n = 1$. We use the complex described in Lemma 4.1.

According to Lemma 4.2 (cf. relations (9)) together with the basic property of the multi-filtration (Proposition 2.8), the chain complex admits a subcomplex generated by CF_3 and DF_3. Indeed, the homology of this complex is trivial, in view of Eq. (11). Thus, $\widehat{HFK}(C_{r,1}, 2r-1)$ is calculated as the homology of the induced quotient complex. Another application of this principle allows us to cancel also the generators CE and DE. The leftover complex, generated by CF_1, CF_2, DF_1, and DF_2, now admits a quotient complex which is generated by CF_1 and DF_1 and hence, according to Eq. (11), has trivial homology. (Note that this step is skipped when $r = 2$.)

Thus, $\widehat{HFK}(C_{r,1}, 2r-1)$ is calculated by the homology of the remaining complex generated by CF_2 and DF_2. Since $CF_2 \not\cong DF_2$, it follows that the homology is

$$\mathbb{Z}_{(2r-1)} \oplus \mathbb{Z}_{(2r)},$$

verifying the calculation of $\widehat{HFK}(C_{r,n}, 2r-1)$ when $n = 1$.

Note that for the pictured knot projection, are two states representing filtration level $2r+1$ (and none representing higher filtration levels). However, these two states are quickly seen to cancel (they, too, are connected by a quadrilateral).

To go from $n = 1$ to arbitrary n, observe that $C_{r,0}$ is an unknot. Thus, we have a skein exact sequence relating the various Conway knots, corresponding to Eq. (12):

$$\cdots \to \widehat{HFK}(C_{r,n-1}, i) \xrightarrow{f_1^n} \widehat{HFK}(Y(r), i) \xrightarrow{f_2^n} \widehat{HFK}(C_{r,n}, i) \to \cdots, \tag{12}$$

for any integer i, where now $Y(r)$ is an oriented $(r+1, -r, -r-1, r)$ pretzel link, rather than the pretzel link $(r+1, -r, r, -r-1)$ belonging to the Kinoshita–Terasaka knots considered earlier. (Of course, $Y(r)$ is a mutant of $X(r)$, and both have trivial Alexander polynomial.)

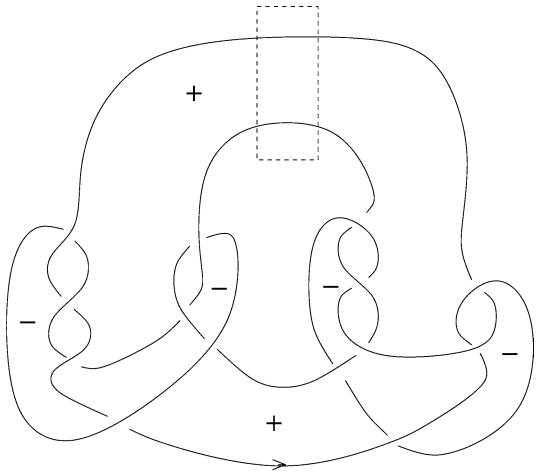

Fig. 11. *A Seifert surface*. We have illustrated here a genus $2r-2$ Seifert surface for the $(r+1, -r, -r-1, r)$ pretzel link, when $r = 2$. A Seifert surface for the Conway knot is obtained as a Murasugi sum with the cylinder (with n full twists) at the indicated (dashed) rectangle.

With these remarks in place, the induction used to verify the theorem runs exactly as it did in the case of $KT_{r,n}$. As a consequence, we also obtain the following formula for $Y(r)$:

$$\widehat{HFK}\big(Y(r), 2r-1\big) \cong \mathbb{Z}_{(2r-\frac{1}{2})} \oplus \mathbb{Z}_{(2r+\frac{1}{2})}. \qquad \square$$

4.1. A Seifert surface

Note that the Conway knot $C_{r,n}$ has a genus $2r-1$ Seifert surface, obtained by a straightforward modification of the picture for the case where $r=2, n=1$ described in [3].

We describe first the Seifert surface for the $(r+1, -r, -r-1, r)$ pretzel link. We "pull down" the overcrossing which connects the first two tassles and the undercrossing which connects the second two. And then, we consider the black regions for the knot projection. Those in turn we label with signs, with the rule that no two regions which meet at a vertex have the same sign. The Seifert surface for this pretzel link is obtained by connecting these black regions by half-twists at each vertex. It is easy to see that the surface F obtained in this manner is orientable, and has $\chi(F) = 4-4r$. We have illustrated this data in Fig. 11 for the case where $r=2$.

We can plumb this with a cylinder with n full twists in it (i.e., forming a Murasugi sum), to obtain a Seifert surface for the Conway knot whose genus is $2r-1$.

5. Calculations for the pretzel knots

In this section, we consider the family of pretzel knots $P(p,q,r)$, where p, q and r are odd. We follow the usual conventions from knot theory here (cf. [10]) for the direction of the twisting (which, unfortunately, seems to be opposite from the convention used in [12]), compare Fig. 12.

There are some relations amongst the pretzel knots. For example, it is easy to see that $P(p,q,r) = P(q,r,p)$, and that $P(-1,1,r)$ is the unknot, for any r.

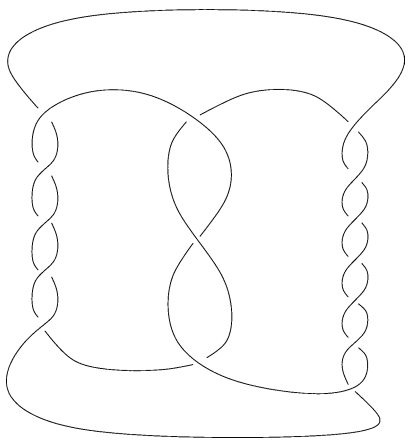

Fig. 12. *The pretzel knot* $P(5,-3,7)$. This knot has trivial Alexander polynomial.

Recall that

$$\Delta_{P(p,q,r)}(T) = \frac{1}{4}\big((pq+qr+pr)\big(T-2+T^{-1}\big)+\big(T+2+T^{-1}\big)\big);$$

thus, there are infinitely many examples with trivial Alexander polynomial. When p, q, and r are all positive, then the signature of $P(p,q,r)$ is given by

$$\sigma\big(P(p,q,r)\big) = 2.$$

When m is an even integer, $T_{2,m}$ denote the torus link, oriented so that the two strands—which we can think of as supported inside a solid torus—are oriented so that the algebraic intersection of $T_{2,m}$ with a disk transverse to the solid torus is zero. In this case,

$$\Delta_{T_{2,m}} = \frac{m}{2}\big(T^{-1/2}-T^{1/2}\big).$$

Moreover, the signature of $T_{2,m}$ is ± 1, depending on the sign of m:

$$\sigma(T_{2,m}) = \operatorname{sgn}(m).$$

Clearly, if we resolve one of the intersection points corresponding to the first strand in $P(p,q,r)$, we obtain the torus link $T_{2,q+r}$. Thus, the skein long exact sequence of [18] in this case gives

$$\cdots \to \widehat{HFK}\big(P(p,q,r)\big) \xrightarrow{F} \widehat{HFK}(T_{2,q+r}) \xrightarrow{G} \widehat{HFK}\big(P(p-2,q,r)\big) \xrightarrow{H} \cdots, \tag{13}$$

where here F and G preserve filtration levels, and both drop absolute grading by $\frac{1}{2}$. The map H also preserves filtration level, and it preserves the parity of absolute grading.

When p, q, and r all have the same sign, then the usual projection of $P(p,q,r)$ is alternating. In this case, the knot Floer homology is determined by [17]. Specifically, in [17], it is shown that if L is a non-split, oriented, alternating link with signature $\sigma = \sigma(L)$, and Alexander–Conway polynomial $\Delta_L(T)$, then if we write

$$\big(T^{-1/2}-T^{1/2}\big)^{n-1}\cdot\Delta_L(T) = a_0 + \sum_{s>0} a_s\big(T^s+T^{-s}\big),$$

then

$$\widehat{HFK}(L,s) \cong \mathbb{Z}^{|a_s|}_{(s+\frac{\sigma}{2})}. \tag{14}$$

Thus, by reflecting $P(p,q,r)$ knot if necessary, we are left with the case where $q<0$ and $p,r>0$. Note that when $m \neq 0$, $T_{2,m}$ is a non-split, alternating link.

Proposition 5.1. *Consider the pretzel knot $K = P(2a+1,-(2b+1),2c+1)$ with $a,b,c \geqslant 0$. Then, if $b \geqslant \min(a,c)$, we have that*

$$\widehat{HFK}(K,1) = \mathbb{Z}^{ab+bc+b-ac}_{(1)}.$$

Proof. For fixed $b \geqslant 0$, we prove the result by induction on both a and c.

Consider the base case where $a = c = 0$. Using the skein exact sequence in the form of Eq. (13) with $p = r = 1$, and the relation that $P(-1, q, 1)$ is the unknot, we see at once that

$$\widehat{HFK}_*\big(P\big(1, -(2b+1), 1\big), 1\big) \cong \widehat{HFK}_{*+\frac{1}{2}}(T_{2,-2b}).$$

Moreover, since $T_{2,-2b}$ is alternating, Theorem 1.4 of [17] applies, and hence, in this case Eq. (14) specializes to give

$$\widehat{HFK}(T_{2,-2b}, 1) \cong \mathbb{Z}^b_{(\frac{1}{2})}.$$

For the inductive step on a, suppose we know the result for $P(2a+1, -2b-1, 2c+1)$, and suppose that $b \geqslant a+1$ and $b \geqslant c$. The condition that $b \geqslant c$ ensures that $T_{2,-2(b-c)+1}$ still has signature -1, and hence $\widehat{HFK}(T_{2,-2(b-c)+1}, 1)$ is supported in dimension $1/2$; by the inductive hypothesis, $\widehat{HFK}(P(2a+1, -2b-1, 2c+1), 1)$ is supported in dimension 1. Thus, the skein exact sequence forces $\widehat{HFK}(P(2a+3, -2b-1, 2c+1), 1)$ to be supported in dimension one. The inductive step on c works analogously. □

We now turn to the case where $b \leqslant \min(a, c)$.

Lemma 5.2. *Let K be the pretzel knot $K = P(2a+1, -2b-1, 2c+1)$ with $a, b, c \geqslant 0$ and $b \leqslant \min(a, c)$. Then,*

$$\operatorname{rk} \widehat{HFK}_{\leqslant 1}(K, 1) \leqslant b(b+1).$$

Proof. This is proven by induction on a and c, starting with the basic case where $\min(a, c) = b$. Suppose for concreteness that $b = c$. Then, it is easy to see that $\operatorname{rk}\widehat{HFK}(P(2a+1, -2b-1, 2b+1), 1)$ is independent of a: the middle term in the skein exact sequence (Eq. (13)) vanishes: it corresponds to $\widehat{HFK}$ of the two-component unlink, whose knot Floer homology is supported in filtration level zero. Thus, it can be calculated in the case where $a < b$, so Proposition 5.1 applies, proving that $\widehat{HFK}(K, 1)$ is supported entirely in dimension one, where its rank is precisely $b(b+1)$.

For the inductive step, suppose we are increasing a by one, and apply Eq. (13). Now, the middle term $T_{2,2(c-b)}$ has signature $+1$, and hence $\widehat{HFK}(T_{2,2(c-b)}, 1)$ is supported in dimension $3/2$. In particular, the map

$$\begin{aligned} H : \widehat{HFK}_{\leqslant 1}\big(P(2a+1, -2b-1, 2c+1), 1\big) \\ \to \widehat{HFK}_{\leqslant 1}\big(P(2a+3, -2b-1, 2c+1), 1\big) \end{aligned}$$

is surjective, providing the inductive step for increasing a. Increasing c follows similarly. □

To proceed, we use a decorated knot projection for $P(2a+1, -2b-1, 2c+1)$, and consider the multi-filtration on states from Section 2.

Specifically, choose a knot projection for $P(2a+1, -2b-1, 2c+1)$ whose corresponding black graph consists of two vertices with degree three, connected by three linear strands

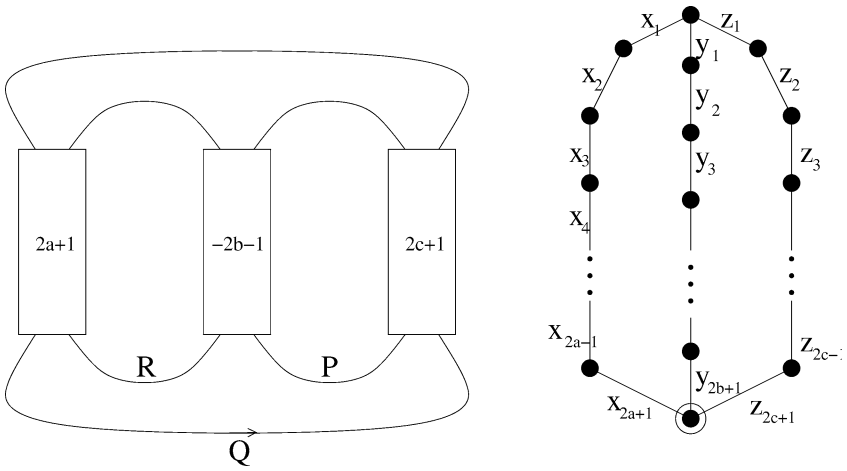

Fig. 13. *Labellings for the pretzel knot* $P(2a+1,-2b-1,2c+1)$. At left, we have a projection for the pretzel knot $P(2a+1,-2b-1,2c+1)$ where, of course, the labeled rectangles represent tangles with a specified number of twists in them. The edges P, Q, R are labeled here. At the right, we have the corresponding black graph (for one of the two colorings). The circled vertex corresponds to the black region distinguished by the edge Q.

of edges $\{x_i\}_{i=1}^{2a+1}$, $\{y_j\}_{j=1}^{2b+1}$, and $\{z_k\}_{k=1}^{2c+1}$. The vertex meeting the edges x_{2a+1}, y_{2b+1}, and z_{2c+1} is the distinguished black vertex. The corresponding distinguished black region is a triangle with three edges P, Q, and R, with P facing the vertex corresponding to x_{2a+1}, Q facing from y_{2b+1}, and R facing z_{2c+1}. Our distinguished edge for the decorated knot projection is Q.

Let $A_{i,j}$ respectively $B_{i,j}$, respectively $C_{i,j}$ be the Kauffman state corresponding to the tree which is obtained by deleting y_i and z_j respectively x_i and z_j respectively x_i and y_j from the black graph.

Lemma 5.3. *For the pretzel knot* $K = P(2a+1,-2b-1,2c+1)$ *with* $a,b,c \geqslant 0$, *the generators of* $\widehat{CFK}(K,1)$ *in dimension one are*

$$\{A_{2i,2j+1}\}_{\substack{1\leqslant i\leqslant b\\ 1\leqslant j\leqslant c}},\ \{C_{2i,2j+1}\}_{\substack{1\leqslant i\leqslant a\\ 1\leqslant j\leqslant b}}$$

and the generators in dimension two are of the form

$$\{B_{2i,2j+1}\}_{\substack{1\leqslant i\leqslant a\\ 1\leqslant j\leqslant c}}.$$

There are no other generators of $\widehat{CFK}(K,1)$.

Proof. This follows at once from the above diagram. □

Lemma 5.4. *For the marked edges* P *and* R, *we have that*

$$M_{B_{2i,2j+1}}(P) - M_{A_{2s,2t+1}}(P) = 2(j-s-t, j-s-t),$$
$$M_{B_{2i,2j+1}}(R) - M_{C_{2s,2t+1}}(R) = 2(i-s-t, i-s-t).$$

Proof. This, too, follows quickly from the diagram. □

Lemma 5.5. *For the pretzel knot $P(2a+1,-2b-1,2c+1)$ with $a,b,c\geqslant 0$, we have that* $\mathrm{rk}\widehat{HFK}_1(P(2a+1,-2b-1,2c+1),1)\geqslant b\cdot(b+1)$.

Proof. According to Lemma 5.4 (together with Proposition 2.8), the generators $A_{2s,2t+1}$ (where $0\leqslant s\leqslant b$ and $0\leqslant t\leqslant c$) with $s+t>2c+1$, of which there are $b(b+1)/2$, all lie in the cokernel of the boundary operator. Similarly, the generators $C_{2s,2t+1}$ (where $0\leqslant s\leqslant a$ and $0\leqslant t\leqslant b$) with $s+t>2a$, of which there are another $b(b+1)/2$, all lie in the cokernel of the boundary operator. Since there are no generators in dimension zero (according to Lemma 5.3), the stated bound follows. □

Proof of Theorem 1.3. The case where $b\geqslant\min(a,c)$ is established in Proposition 5.1. Together, Lemmas 5.2 and 5.5 show that $\mathrm{rk}\widehat{HFK}(P(2a+1,-2b-1,2c+1))=b(b+1)$. The rest of the theorem now follows at once from Lemma 5.3. □

To prove Corollary 1.5, we need the following result, which closely follows [19]:

Proposition 5.6. *Let K be a knot with* $\deg\widehat{HFK}(S^3,K)=1$. *Then, if*

$$\mathrm{rk}\widehat{HFK}_{\mathrm{ev}}\bigl(S^3,K,1\bigr)\geqslant 2\quad\textit{and}\quad\mathrm{rk}\widehat{HFK}_{\mathrm{odd}}\bigl(S^3,K,1\bigr)\geqslant 1,$$

then no integral surgery of S^3 along K is a Seifert fibered space.

Proof. By reflecting the knot if necessary, we can assume that $S^3_p(K)$ is Seifert fibered for some $p\geqslant 0$.

According to Lemma 4.1 of [19],

$$HF^+_{\mathrm{red,ev}}\bigl(S^3_0(K),0\bigr)\cong\widehat{HFK}_{\mathrm{odd}}\bigl(S^3,K,1\bigr).$$

This completes the case where $p=0$, see for example Theorem 3.4 of [19].

As in the proof of Lemma 3.1 of [19], Section 4 of [18] gives a $\mathbb{Z}[U]$-submodule of $HF^+(S^3_n(K),[0])$ (for sufficiently large n) which is isomorphic to $\widehat{HFK}(S^3,K,1)$; indeed, we have a short exact sequence:

$$0\to\widehat{HFK}\bigl(S^3,K,1\bigr)\to HF^+\bigl(S^3_n(K),[0]\bigr)\to HF^+\bigl(S^3\bigr)\to 0.$$

The above is a map of U-modules, and the U action on $\widehat{HFK}(S^3,K,1)$ is trivial. It follows now that

$$\mathrm{rk}HF^+_{\mathrm{red,ev}}\bigl(S^3_n(K)\bigr)\geqslant\mathrm{rk}\widehat{HFK}_{\mathrm{ev}}\bigl(S^3,K,1\bigr)-1,$$
$$\mathrm{rk}HF^+_{\mathrm{red,odd}}\bigl(S^3_n(K)\bigr)\geqslant\mathrm{rk}\widehat{HFK}_{\mathrm{odd}}\bigl(S^3,K,1\bigr).$$

Considering the integer surgeries long exact sequence, it follows that for all $p>0$

$$\mathrm{rk}HF^+_{\mathrm{red,odd}}\bigl(S^3_n(K)\bigr)=\mathrm{rk}HF^+_{\mathrm{red,ev}}\bigl(S^3_p(K)\bigr),$$
$$\mathrm{rk}HF^+_{\mathrm{red,ev}}\bigl(S^3_n(K)\bigr)=\mathrm{rk}HF^+_{\mathrm{red,odd}}\bigl(S^3_p(K)\bigr).$$

In view of our hypotheses, then $HF^+_{\mathrm{red}}(S^3_p(K))$ is non-trivial in both even and odd degrees. On the other hand, results from [20] show that for a Seifert fibered space with $b_1(Y)=0$, $HF^+_{\mathrm{red}}(Y)$ is supported in either even or odd degrees (this is proved in Corollary 1.4 of [20] when $b_1(Y)=0$. □

Proof of Corollary 1.5. This is a direct consequence of Theorem 1.3 and Proposition 5.6. □

6. Knots with few crossings

We give here another application of the results of Proposition 2.6, showing that the Floer homology groups of all but two of the knots with nine or fewer crossings behave like the Floer homology of alternating knots. The two counterexamples to this are the $(3,4)$-torus knot (which appears in the tables under the name 8_{19}) and a certain nine-crossing knot 9_{42}. In fact, the knot Floer homologies of these two knots have been determined in Theorem 1.2 of [16] and Proposition 6.6 of [18], respectively, where it is shown that:

$$\widehat{HFK}(8_{19},i)\cong\begin{cases}\mathbb{Z}_{(0)} & \text{if } i=3,\\ \mathbb{Z}_{(-1)} & \text{if } i=2,\\ \mathbb{Z}_{(-4)} & \text{if } i=0,\\ \mathbb{Z}_{(-5)} & \text{if } i=-2,\\ \mathbb{Z}_{(-6)} & \text{if } i=-3,\\ 0 & \text{otherwise,}\end{cases}$$

$$\widehat{HFK}(9_{42},i)\cong\begin{cases}\mathbb{Z}_{(1)} & \text{if } i=2,\\ \mathbb{Z}^2_{(0)} & \text{if } i=1,\\ \mathbb{Z}^2_{(-1)}\oplus\mathbb{Z}_{(0)} & \text{if } i=0,\\ \mathbb{Z}^2_{(-2)} & \text{if } i=-1,\\ \mathbb{Z}_{(-3)} & \text{if } i=-2,\\ 0 & \text{otherwise.}\end{cases}$$

(Note that the standard knot tables do not distinguish a knot from its mirror. For the above statements, we have chosen the versions of the knots whose signature is negative.)

Theorem 6.1. *Except for the knots* 8_{19} *and* 9_{42}*, any other knot* K *admitting a projection with nine or fewer crossings has the property that*

$$\widehat{HFK}(K,i)\cong\mathbb{Z}^{|a_i|}_{(i+\frac{\sigma}{2})}, \tag{15}$$

where here σ *denotes the signature of the knot* K*, and the* a_i *are the coefficients of its symmetrized Alexander polynomial.*

Proof. Of course, for alternating knots, the theorem follows from [17]. Now, there are only nine non-alternating knots to consider here according to standard knot tables, see, for example, [1]. One of these, the knot 9_{46}, which is the pretzel knot $P(-3,3,3)$, will be

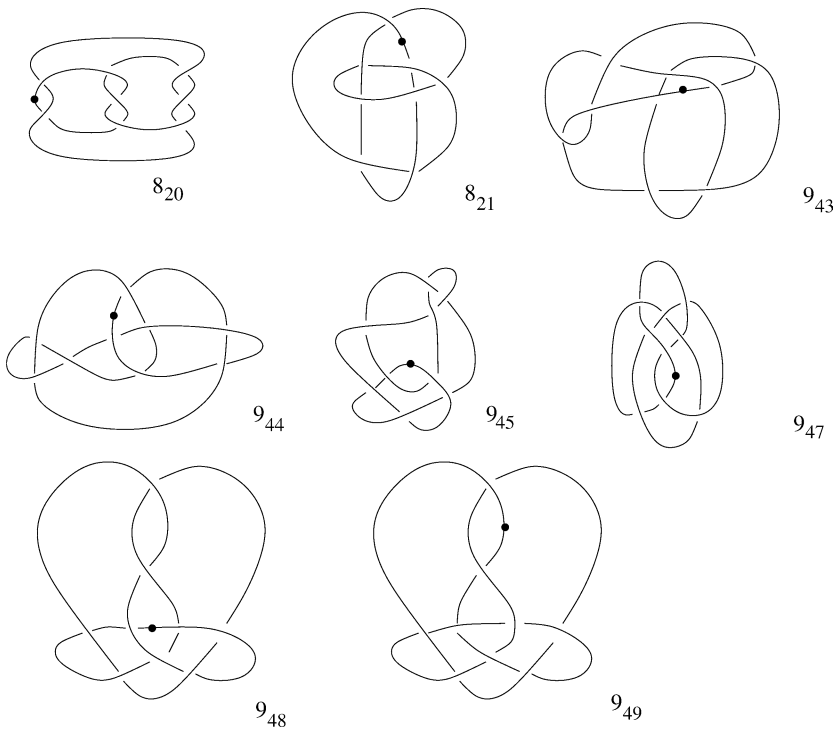

Fig. 14. *Decorated knot projections for small knots*. We have illustrated here knots with nine or fewer crossing which do not admit alternating projections, except for 8_{19} (the $(3,4)$ torus knot), 9_{42}, and 9_{46} (the pretzel knot $P(-3,3,3)$).

handled separately. We illustrate distinguished edges for knot projections for the remaining eight knots in Fig. 14 (but dropping orientations).

Now, of these eight, we consider 9_{43} separately as well. For the remaining seven knots, it is straightforward to see that in each filtration level, all of the essential states have the same absolute grading. Indeed, calculating these absolute gradings, one can readily verify that for these knots, the essential states with filtration level i all have absolute grading $i + \sigma/2$. In view of Proposition 2.6, the theorem then follows for these seven knots.

For the case of 9_{43}, a direct analysis using the illustrated decorated knot projection verifies Eq. (15) for all $i < 0$, and hence also for all $i \neq 0$, in view of the symmetry of $\widehat{HFK}$, Eq. (2). In the case where $i = 0$, now, we claim that there are three generators, one in dimension -1, and two in dimension -2. In fact, a closer look at the states reveals that the essential state X in dimension -1 can be connected to an essential state Y in dimension -2 by a homotopy class ϕ whose associated domain is an octagon (with multiplicity $+1$, missing the reference point z). Compare with the genus four Heegaard diagram of S^3 pictured in Fig. 16, where there are three generators for S^3, A_1, A_2, B, with homotopy classes connecting A_1 respectively A_2 to B represented by octagons. It now follows easily that for a homotopy class ϕ whose domain is an octagon,

$$\#\big(\mathcal{M}(\phi)/\mathbb{R}\big) = \pm 1.$$

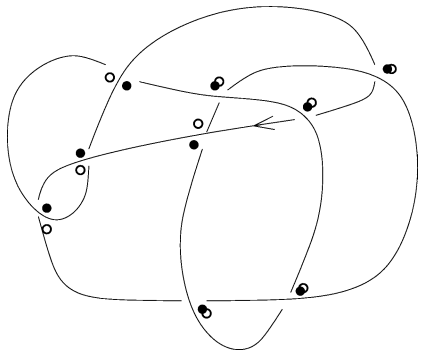

Fig. 15. *A differential for* 9_{43}. We have illustrated here two of the essential states X and Y for the indicated decorated knot projection (where the distinguished edge is the one containing the arrow). The state X is represented by the collection of dark circles, while Y is represented by the hollow circles. Moreover, X and Y are in dimensions -1 and -2, respectively, and it is easy to see that the domain of the homotopy class connecting X to Y is an octagon.

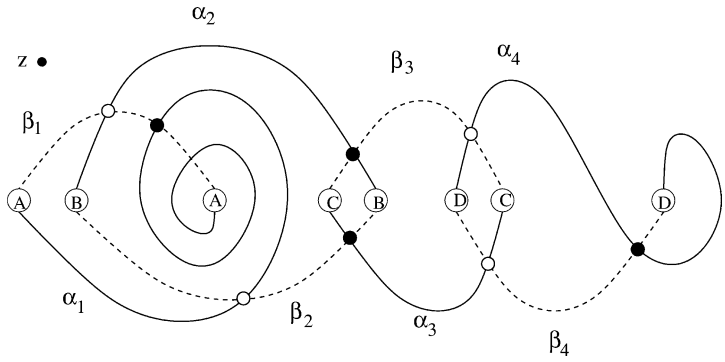

Fig. 16. *Octagons*. In this genus four Heegaard diagram for S^3, there are three generators for $\widehat{CF}(S^3)$. Two of them are indicated here—one by the unmarked solid circles (call it X), the other by the unmarked hollow circles (call that Y). It is easy to find an octagonal domain $\mathcal{D}(\phi)$ with $n_z(\phi) = 0$ which connects X to Y (and indeed there is another octagonal domain connecting the other intersection point X' to Y). This forces $\#\mathcal{M}(\phi)/\mathbb{R} = \pm 1$.

Hence, we have that the boundary operator in $\widehat{CFK}(9_{43}, 0)$ is non-trivial, and indeed that the homology in filtration level 0 is given by $\mathbb{Z}_{(-2)}$, completing the verification of Eq. (15) for 9_{43}.

Finally, we turn to the pretzel knot $P(-3,3,3)$. As in Section 5, we fit this into a skein exact sequence

$$\cdots \to \widehat{HFK}\big(P(-3,3,3)\big) \xrightarrow{F} \widehat{HFK}(U_2) \xrightarrow{G} \widehat{HFK}\big(P(-3,3,1)\big) \xrightarrow{H} \cdots,$$

where here U_2 is the unlink with two components (this is $T_{2,0}$ in the notation from Section 5). By using the action of the homology class which links, it is easy to see that $\widehat{HFK}(P(-3,3,3)) \cong \widehat{HFK}(P(-3,3,1))$. Note that $P(-3,3,1) = P(-1,-1,5) = P(1,1,3)$, which alternates. □

References

[1] G. Burde, H. Zieschang, Knots, in: de Gruyter Stud. Math., vol. 5, de Gruyter, Berlin, 1985.
[2] E. Eftekhary, Heegaard Floer homologies for pretzel knots, math.GT/0311419.
[3] D. Gabai, Foliations and genera of links, Topology 23 (4) (1984) 381–394.
[4] D. Gabai, Genera of the arborescent links, Mem. Amer. Math. Soc. 59 (1986), i–viii and 1–98.
[5] H. Goda, M. Teragaito, Dehn surgeries on knots which yield lens spaces and genera of knots, Math. Proc. Cambridge Philos. Soc. 129 (3) (2000) 501–515.
[6] L.H. Kauffman, Formal Knot Theory, in: Math. Notes, vol. 30, Princeton University Press, Princeton, NJ, 1983.
[7] M. Khovanov, A categorification of the Jones polynomial, Duke Math. J. 101 (2000) 359–426.
[8] S. Kinoshita, H. Terasaka, On unions of knots, Osaka Math. J. 9 (1957) 131–153.
[9] P.B. Kronheimer, T.S. Mrowka, Scalar curvature and the Thurston norm, Math. Res. Lett. 4 (6) (1997) 931–937.
[10] W.B.R. Lickorish, An Introduction to Knot Theory, in: Graduate Texts in Math., vol. 175, Springer, Berlin, 1997.
[11] T.W. Mattman, The Culler–Shalen seminorms of the $(-2, 3, n)$ pretzel knot, math.GT/9911085.
[12] P.S. Ozsváth, Z. Szabó, Absolutely graded Floer homologies and intersection forms for four-manifolds with boundary, Adv. in Math. 173 (2003) 179–261.
[13] P.S. Ozsváth, Z. Szabó, Holomorphic disks and three-manifold invariants: Properties and applications, math.SG/0105202.
[14] P.S. Ozsváth, Z. Szabó, Holomorphic disks and topological invariants for closed three-manifolds, math.SG/0101206.
[15] P.S. Ozsváth, Z. Szabó, Holomorphic triangles and invariants for smooth four-manifolds, math.SG/0110169.
[16] P.S. Ozsváth, Z. Szabó, On knot Floer homology and lens space surgeries, math.GT/0303017.
[17] P.S. Ozsváth, Z. Szabó, Heegaard Floer homology and alternating knots, Geom. Topology 7 (2003) 225–254.
[18] P.S. Ozsváth, Z. Szabó, Holomorphic disks and knot invariants, math.GT/0209056.
[19] P.S. Ozsváth, Z. Szabó, On Heegaard Floer homology and Seifert fibered surgeries, math.SG/0301026.
[20] P.S. Ozsváth, Z. Szabó, On the Floer homology of plumbed three-manifolds, Geom. Topology 7 (2003) 185–224.
[21] J. Rasmussen, Floer homologies of surgeries on two-bridge knots, Algebr. Geom. Topology 2 (2002) 757–789.
[22] J. Rasmussen, Floer homology and knot complements, Ph.D. Thesis, Harvard University, 2003.
[23] S.M. Wehrli, Khovanov homology and Conway mutation, math.GT/0301312.